Ecotoxicology and Environmental Safety 159 (2018) 272–283

Contents lists available at ScienceDirect

Ecotoxicology and Environmental Safety

journal homepage: www.elsevier.com/locate/ecoenv

Physiological, ultrastructural, biochemical and molecular responses of young cocoa plants to the toxicity of Cr (III) in soil

Junea Leandro do Nascimento[a], Alex-Alan Furtado de Almeida[a,*], Joedson P. Barroso[a], Pedro A.O. Mangabeira[a], Dário Ahnert[a], Artur G.R. Sousa[a], José Vitor S. Silva[a], Virupax C. Baligar[b]

[a] State University of Santa Cruz, Department of Biological Sciences, Rodovia Jorge Amado, km 16, 45662-900 Ilhéus, BA, Brazil
[b] USDA-ARS-Beltsville Agricultural Research Center, Beltsville, MD, USA

ARTICLE INFO

Keywords:
Theobroma cacao
Oxidative stress
Gene expression
Hormesis
Proline
Autophagy

ABSTRACT

The objective of this study was to evaluate Cr toxicity in young plants of the CCN 51 *Theobroma cacao* genotype at different concentrations of Cr^{3+} in the soil (0, 100, 200, 400 and 600 mg kg^{-1}) through physiological, ultrastructural, antioxidant and molecular changes. Doses of 400 and 600 mg Cr^{3+} kg^{-1} soil severely affected foliar gas exchange, promoted by damages in photosynthetic machinery evidenced by the decrease in CO_2 fixation. Decreased expression of *psbA* and *psbO* genes, changes in enzymatic activity and lipid peroxidation also affected leaf gas exchange. A hormesis effect was observed at 100 mg Cr^{3+} kg^{-1} soil for the photosynthetic activity. As a metal exclusion response, the roots of the cocoa plants immobilized, on average, 75% of the total Cr absorbed. Ultrastructural changes in leaf mesophyll and roots, with destruction of mitochondria, plasmolysis and formation of vesicles, were related to the oxidative stress promoted by excess ROS. The activity of the antioxidant enzymes SOD, APX, GPX and CAT and the amino acid proline coincided with the greater expression of the *sod cyt* gene demonstrating synchronicity in the elimination of ROS. It was concluded, therefore, that the tolerance of the cocoa plants to the toxicity of Cr^{3+} depends on the concentration and time of exposure to the metal. Higher doses of Cr^{3+} in the soil promoted irreversible damage to the photosynthetic machinery and the cellular ultrastructure, interfering in the enzymatic and non-enzymatic systems related to oxidative stress and gene expression. However, the low mobility of the metal to the leaf is presented as a strategy of tolerance to Cr^{3+}.

1. Introduction

Theobroma cacao L. is a tropical crop of high importance, mainly due to the commercial value of its beans. The beans are ground for the preparation of products such as cocoa butter, jellies, liqueurs, cosmetics, chocolate, etc. (Almeida et al., 2014; Almeida and Valle, 2009). Due to the high concentration of fats, carbohydrates, polyphenols and antioxidants, in addition to benefits provided to human health, cocoa by-products are much appreciated and even are considered as a luxury items (Bertoldi et al., 2016). The CCN 51 (Colección Castro Naranjal) cultivar has become the preferred one among the producers due to its high productivity, tolerance to climatic variations and pathogens (Boza et al., 2014; Herrmann et al., 2015). Recent studies have reported the presence of traces of various heavy metals, including chromium (Cr) in beans and cocoa by-products such as chocolate (Arévalo-Gardini et al., 2017; Bertoldi et al., 2016; Yanus et al., 2014), with a positive linear correlation between Cr concentration in the beans and by-products (Yanus et al., 2014).

The most common and stable forms of Cr on the Earth's surface are Cr^{3+} (trivalent) and Cr^{6+} (hexavalent), which differ from each other in terms of soil mobility, bioavailability and toxicity to plants (Ashraf et al., 2017; Panda and Choudhury, 2005). In the soil solution, Cr is made available to plants by weathering the original rock and is around 10 e 100 mg kg^{-1} soil (Kabata-Pendias, 2011). However, the increase of its concentration in soil and availability also occurs by anthropogenic actions, such as the production of metallic alloys, leather, electroplating and pigments (Gomes et al., 2017; Hasan et al., 2017), as well as chemical fertilizers and sewage sludge (Hayat et al., 2012; Srivastava et al., 2017).

There are no reports that Cr^{3+} has any essential function in plant metabolism or on its specific mechanisms of absorption (Oliveira, 2012). Recently its essentiality in human and animal health has been

* Corresponding author.
E-mail address: alexalan.uesc@gmail.com (A.-A.F. de Almeida).

https://doi.org/10.1016/j.ecoenv.2018.04.058
Received 19 December 2017; Received in revised form 18 April 2018; Accepted 26 April 2018

questioned (Vicent, 2017). However, at low concentrations beneficial effects have been reported in some plant species such as *Allium cepa, Mentha citrata* and *Solanum nigrum* (Patnaik et al., 2013; Prasad et al., 2010; UdDin et al., 2015). At high soil concentrations, Cr can accumulate in plant tissues, preferably in the roots (Shanker et al., 2005), promoting toxic effects and thus establishing a bi-phasic dose-response process called hormesis. According to hormesis concepts a contaminating substance applied at low doses may exert a beneficial or stimulatory action, whereas, applied at high doses, it will exert a deleterious and inhibitory action (Calabrese and Blain, 2009; Calabrese, 2015; Poschenrieder et al., 2013).

High dosages of Cr^{3+} in plant tissues may promote molecular, biochemical and ultrastructural changes. As a result of the damage to cell membranes, alteration of chloroplasts, reductions in photosynthetic activity, degradation of chloroplastidic pigments and induction oxidative stress with excessive formation of reactive oxygen species (ROS) are observed, which can lead to senescence (Afshan et al., 2015; Scoccianti et al., 2016). Overproduction of ROS may result in imbalance in cellular homeostasis, inducing the formation of antioxidative enzymes, preferably at their sites of production (Hossain et al., 2012), as a mechanism of ROS elimination and cellular detoxification (Gomes et al., 2017). In addition, may promote lipid peroxidation (Shahid et al., 2017) and in some cases autophagy (Farah et al., 2016). In autophagy, autophagosomes (specialized organelles) sequester cytoplasmic components including metals, forming vesicles, which fuse with the vacuole (Hasan et al., 2017). However, if induced in large quantities autophagosomes can act as initiator or executor of programmed cell death (Minina et al., 2014). In addition to enzymes, increases in the synthesis and accumulation of non-enzymatic osmolytes, such as proline, have also been reported in the elimination of ROS induced by heavy metals (Tripathi et al., 2013) and also by Cr^{3+} (Anjum et al., 2017; Tang et al., 2012). Proline has multiple functions, such as free radical scavenger, enzyme, membrane and protein structure stabilizer and helps to maintain the cytosolic pH and the equilibrium of the redox reactions of the cells (Aslam et al., 2017).

Another important mechanism of detoxification and tolerance of plants against Cr and other heavy metals stress is chelation of the metal, with peptides such as phytochelatins (*phyt*) and metallothioneins (*Mt2b*) (Hasan et al., 2017; Srivastava et al., 2017). The biosynthesis of both peptides is stimulated as a function of the free metal concentration in the cells, however phytochelatin synthesis occurs more rapidly in response to stress. Both acts in the Cr sequester, inactivating the metal in the cytoplasm and transporting the Cr-protein complexes to the vacuoles, where they are compartmentalized, making them incapable of damaging the plants (Gomes et al., 2017; Hasan et al., 2017). Phytochelatins are synthesized by the enzyme *phytochelatin synthase* using reduced glutathione (GSH) as a substrate (Taiz et al., 2017). Metallothioneins are low-molecular-weight, cysteine-rich proteins, which give them high affinity for metal ions (Hasan et al., 2017; Shahid et al., 2017).

The purpose of this work was to describe the main defense mechanisms to stress of Cr^{3+} in clonal CCN 51 plants grown in soil as substrate. Contribute to elucidate the intoxication process, aiming to reduce health risks due to the accumulation of Cr in the plants of *T. cacao* and consequent contamination of the food chain by this metal. We examined (i) the physiological changes in plants after exposure to different Cr concentrations, (ii) explored Cr uptake and translocation, (iii) changes in cell ultrastructure in leaves and roots, (iv) the role of cellular antioxidant activities (enzymatic and non-enzymatic) in protecting the plants from Cr-toxicity, (v) the expression of genes associated with the biosynthesis of proteins involved in antioxidative metabolism and in metal chelation. The results may be used in future programs of genetic enhancement.

2. Material and methods

The experiment was conducted in a greenhouse at the State University of Santa Cruz (UESC), Ilhéus, Bahia, Brazil (14° 47 ′S, 39° 13′ W) in the period from 24 July 2015–14 January 2016. Clonal plants of the CCN 51 cacao cultivar were grown on sandy soil as substrate in pots with a capacity of 15 L. The soil was previously liming (pH 5.6) and the plants were fertilizer during planting and biweekly coverage after planting. Treatments without addition of Cr^{3+} (control) and with addition of Cr^{3+} were applied in the form of chromium chloride hexahydrate ($CrCl_3{\cdot}6H_2O$), in the concentrations of 100, 200, 400 and 600 mg Cr^{3+} kg^{-1} soil, (Han et al., 2004; Tang et al., 2012). The plants were obtained by rooting stem cuttings of plagiotropic branches. The stem cuttings were collected from plants with 5–10 years of age, at the Biofábrica de Cacau Institute (IBC, Banco do Pedro, Ilhéus, BA). The treatments with concentrations of Cr^{3+} (100, 200, 400 and 600 mg kg^{-1} soil) were applied in solution (100 mL per pot) on 14/12/2015 in one-year-old *T. cacao* plants. During the acclimation period [24/07/2015–13/12/2015] and during the period of exposure to treatments with Cr^{3+} [14/12/2015–13/01/2016], the plants were irrigated with rainwater, aiming to keep the soil close to field capacity. During the experimental period, photosynthetically active radiation (PAR) was recorded using Hobo S-LIA-M003 light radiation sensors coupled to the Hobo Micro Station Data Logger (Onset Computer, Bourne, MA, USA). Air temperature (T °C) and relative humidity (RH %) were recorded by means of Hobo H8 Pro sensors (Onset, Computer, Bourne, MA, USA) for characterization of cropping environments (Fig. S1). Soil characterization and recommended fertilization were described in Table S1.

2.1. Foliar gas exchanges

During the experimental period, the net photosynthetic rate per unit leaf area (P_N), stomatal conductance to water vapor (*gs*) and leaf transpiration (*E*) were monitored at 1, 4, 8, 15, 21 and 28 days after application of the treatments (AAT) in a completely expanded and mature leaf. Four plants were evaluated per treatment, between 7 and 11 h, using a portable LI-6400 photosynthetic measurement system (Li-Cor, Nebraska, USA) equipped with a 6400-02B RedBlue artificial light source. During the measurements the PAR value was set at 800 μmol photons m^{-2} s^{-1}, above the saturation irradiance without photoinhibition, and the leaf temperature at 26 °C (Rehem et al., 2011a, 2011b). The readings were recorded in the range of 2–3 min (coefficient of variation < 0.3%). The values of P_N, *gs* and *E* were used to calculate the intrinsic water use efficiency (*WUEi*) and instantaneous water use efficiency (*WUE*).

2.2. Photosynthetic pigments

Mature leaves (2nd or 3rd from the apex) of the plants of the various treatments were collected 96 h AAT. Immediately after, they were immersed in liquid nitrogen, stored in ultrafreezer − 80 °C and later lyophilized. Subsequently, the leaves were macerated in liquid nitrogen, 50 mg of leaf tissue was weighed into eppendorf tubes and 2 mL of 80% acetone was added for the extraction of the photosynthetic pigments, according to methodology described by Torres et al. (2006). The absorbances of the extracts were determined using a microplate spectrophotometer (SpectraMax Paradigm Multi-Mode Microplate Reader, Molecular Device, USA), at wavelengths corresponding to 646 nm, 663 nm and 470 nm, for the determination of the concentrations of *Chl a*, *Chl b* and *Car*, respectively, using the equations described by Lichtenthaler and Wellburn (1983) for 80% acetone extracts.

2.3. Total Cr determination

At 30 days AAT, the total Cr concentration was determined in the

leaves and roots of the treatments without and with Cr^{3+} at doses of 100 and 200 mg Cr^{3+} kg^{-1} soil and at 4 days AAT at doses 400 and 600 mg Cr^{3+} kg^{-1} soil. Ten plants were collected per treatment and separated into roots and shoot. The roots were submitted to the following washing sequence: running water, 0.1% neutral detergent solution, distilled water, 3% HCl and distilled water (Souza Junior et al., 2011), aiming at the removal of metals at the root surface and in apparent free space. Soon after, the plants were conditioned in paper bags and taken to a forced air circulation oven at 70 °C until reaching a constant mass. Subsequently, the dry and ground vegetable material was subjected to nitro-perchloric digestion (3: 1 v.v.). After digestion, total Cr was determined by an Inductively-Coupled Plasma Optical Emission Spectrometer (ICP-OES) in a "Varian 710-ES" model (Agilent Technologies, Santa Clara, CA).

2.4. Antioxidant metabolism

The enzymatic assays were performed in foliar tissue (2nd or 3rd leaf from the apex) collected at 3, 6, 12, 24, 48 and 96 h AAT intervals. Immediately after collection, the leaves were immersed in liquid nitrogen, stored in ultrafreezer − 80 °C and then lyophilized. The activity of the enzymes guaiacol peroxidase (GPX, EC 1.11.1.7), ascorbate peroxidase (APX, EC 1.11.1.11), superoxide dismutase (SOD, EC 1.15.1.1), catalase (CAT, EC 1.11.1.6) and glutathione reductase (GR, EC 1.8.1.7), was determined according to Carlberg and Mannervik (1985), Giannopolitis and Ries (1977), Havir and Mchale (1987), Nakano and Asada (1981), Pirovani et al. (2008), respectively.

2.5. Determination of malondialdehyde (MDA)

The lipid peroxidation was obtained by determining the content of reactive substances to thiobarbituric acid, mainly malondialdehyde (MDA), performed according to the protocol described by Cakmak and Horst (1991), with some modifications (Souza et al., 2014). We used part of the collected and lyophilized leaf samples for the determination of the antioxidative metabolism. Absorbance reading was performed at 532 and 600 nm wavelengths on a microplate spectrophotometer (SpectraMax Paradigm Multi-Mode Microplate Reader, Molecular Device, USA). The correction for non-specific turbidity was made by subtracting the absorbance at 600 nm. The MDA concentration was calculated using the absorbance coefficient for the MDA of 155 mM cm^{-1}.

2.6. Proline

The free proline in the leaves of the plants of the various treatments was extracted by the sulfosalicylic acid method and determined in a 520 nm wavelength spectrophotometer according to a protocol described by Bates et al. (1973), with modifications (Khedr et al., 2003). Were used part of the collected and lyophilized leaf samples for the determination of the antioxidative metabolism. 520 nm. The results were expressed as μmoles g^{-1} DW.

2.7. Real-time quantitative PCR

From the results of the analysis of antioxidative metabolism, lipid peroxidation and proline, two collection intervals were selected [24 h and 96 h AAT], where the highest responses of these variables were observed in the different treatments for the analysis of the gene expression. Were used part of the collected and lyophilized leaf samples for the determination of the antioxidative metabolism. RNA extraction was performed using the RNAqueous® kit (Ambion). The RNA samples were treated with DNase I (Thermo Scientific), incubated at 37 °C for 30 min and quality of the RNA was evaluated by electrophoresis in 1% agarose gel. The quantification of RNA (μg mL^{-1}), was performed in spectrophotometer (*NanoDrop 2000c UV–Vis Spectrophotometer Thermo Scientific*), at wavelengths of 260 and 280 nm. Dnase I-treated RNA samples were used for cDNA synthesis using the High Capacity RNA-to-cDNA kit (Applied Biosystems, CA, USA) according to the manufacturer's instructions. The qPCR was performed on an "Applied Biosystems 7500 Real-Time PCR System" thermocycler using non-specific detection sequence (fluorophore) SYBR Green I. The abundance of transcripts was analyzed using specific primers described previously by Araújo et al. (2017), related to the biosynthesis of photosystem 2 (PS2) proteins of the photochemical phase of photosynthesis (*psbA* and *psbO*), antioxidative enzymes (Cu-Zn *sod cyt* and Cu-Zn *sod chl*), biosynthesis of the metallothionein polypeptide (*Mt2b*) and biosynthesis of *phytochelatin synthase* (*phyt*). Reaction mix was composed of 50 ng of cDNA as template, 5 μM of each primer and 6.25 μL of Power SYBR® Green PCR Master Mix. The relative expression numbers of the genes were calculated as the number of times in relation to the control plant using the 2-ΔΔCt method (Livak and Schmittgen, 2001), with the *actin* and *β-tubulin* genes as references.

2.8. Transmission electron microscopy (TEM)

Ultrastructural analyses of cellular organelles in transmission electron microscopy (TEM) were conducted at the Electronic Microscopy Center of the State University of Santa Cruz. At 30 days AAT, ends of primary roots and middle part of mature leaves of control treatments and Cr^{3+} treatments at the concentration of 200 mg Cr^{3+} kg^{-1} soil and at 4 days AAT at the concentration of 600 mg Cr^{3+} kg^{-1} soil were sectioned, collected and prefixed in 2.5% glutaraldehyde, prepared in 0.1 M sodium cocodylate (pH 7.2). Subsequently, sections of roots and leaves were fixed in osmium tetroxide, prepared in the same buffer for 1 h, followed by dehydration in an ethanolic series and included in LR White resin following the methodology described by Castro et al. (2015). Subsequently, ultra-thin sections were obtained using ultramicrotome (Model MS UC6 LEICA Microsystems) and analyzed in TEM Morgani TM-model 268 D (FEI Company).

2.9. Statistical analysis

The experimental design was completely randomized, with 5 treatments, 20 plants per experimental unit (one plant per pot), making a total of 100 plants. The MDA content, proline, enzymes and expression gene data were submitted two-way factorial analyses of variance (ANOVA) with sampling time and treatments as main factors. One-way ANOVA was used to test the treatment effects on leaf gas exchange, photosynthetic pigments and Cr total. Significant differences between means were compared by the Tukey test ($p < 0.01$ and $p < 0.05$) using the "SISVAR" software version 5.6. The data are the means ± SE of four replicates for analyses of foliar gas exchanges, Cr total, enzyme activity and proline, three for ultrastructural analyses, five for malondialdehyde, and six repetitions for the photosynthetic pigments and expression gene. Increases in treatments were calculated according to Abbott (1925).

3. Results

3.1. Leaf gas exchange

Leaf gas exchanges of the CCN 51 cocoa plants were severely affected by Cr^{3+} toxicity in the first 24 h AAT (Fig. 1). At the doses of 200, 400 and 600 mg Cr^{3+} kg^{-1} soil, there were significant reductions ($p < 0.01$) of 77%, 98% and 97% for the photosynthetic rate (P_N) (Fig. 1A), of 36%, 59% and 74% for stomatal conductance (*gs*) (Fig. 1B) and 16%, 59% and 73% for transpiration (*E*) (Fig. 1C), respectively, when compared to the control treatment. At the dose of 100 mg Cr^{3+} kg^{-1} soil the values of P_N and *gs* were significantly higher than the control. At 4 days AAT, significant increase and recovery of P_N, *gs* and *E* at the dose of 200 mg Cr^{3+} kg^{-1} soil were observed, becoming similar

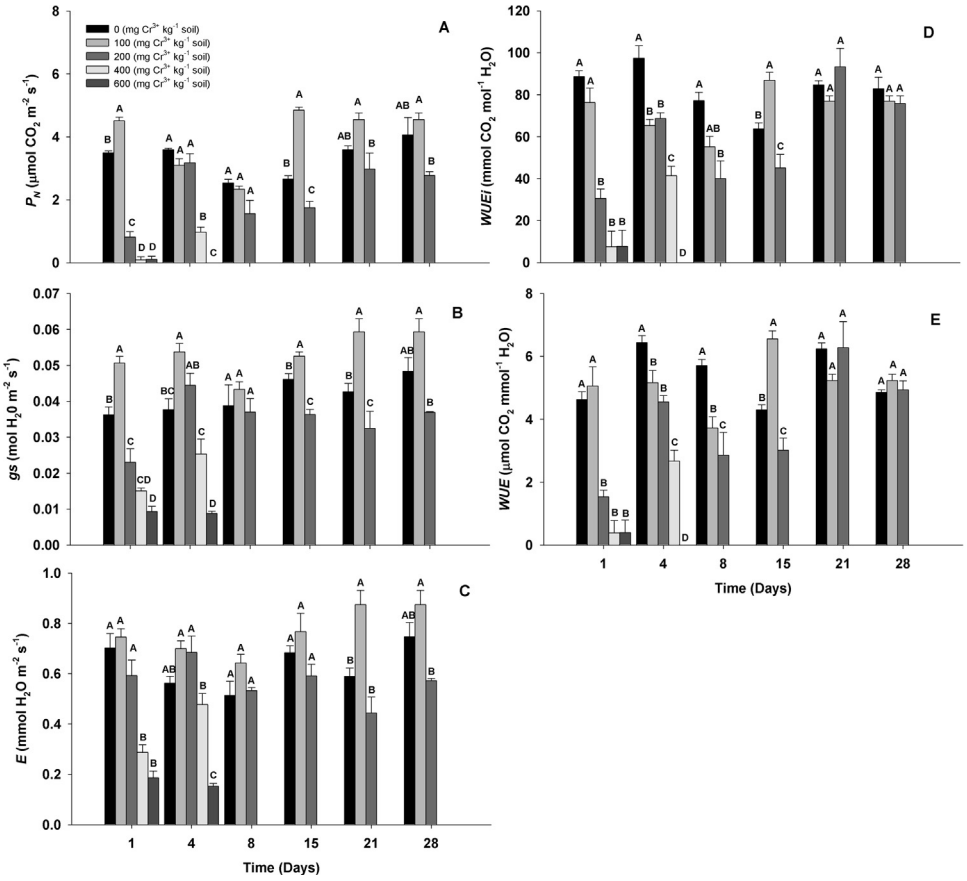

Fig. 1. (A) Photosynthetic rate per unit leaf area (P_N), (B) stomatal conductance to water vapor (*gs*), (C) transpiration (*E*), (D) intrinsic water use efficiency (*WUEi*) and (E) instantaneous water use efficiency (*WUE*) on plant leaves of the clonal CCN 51 cacao genotype submitted to Cr^{3+} stress in the soil for 28 days. Mean values of four biological replicates ± SE. Capital letters indicate averages comparisons between treatments by the Tukey test ($p < 0.01$).

to the control (Fig. 1). On the other hand, in the doses corresponding to 400 and 600 mg Cr^{3+} kg^{-1} soil, the values of P_N were significantly lower than the control with reductions of 73% and 100%, respectively (Fig. 1A). Due to the low recovery of the photosynthetic activity and the low survival rate of the plants (data not shown), the treatments at doses of 400 and 600 mg Cr^{3+} kg^{-1} soil were finalized at 4 days AAT, followed by collecting of plant material for the other analysis. At 15 days AAT, the values of P_N and *gs* were significantly higher in treatment with 100 mg Cr^{3+} kg^{-1} soil (82% and 14%), and lower in the dose of 200 mg Cr^{3+} kg^{-1} soil (34% and 21%) (Fig. 1A). At 21 days AAT, significant increases of *gs* and *E* were observed in the treatment with 100 mg Cr^{3+} kg^{-1} soil, with increases of 39% and 48%, respectively. Significant differences ($P < 0.01$) for the intrinsic (*WUEi*) (Fig. 1D) and instantaneous (*WUE*) (Fig. 1E) efficiency of water use were observed in day 1 AAT up to day 15 AAT assessments. On day 1 AAT treatments with 200, 400 and 600 mg Cr^{3+} kg^{-1} soil reduced the *WUEi* and *WUE* by up to 90%. At 4 days AAT all treatments with Cr^{3+} reduced the *WUEi* and *WUE* by up to 100% when compared to the control treatment. In addition, at 8 days AAT for the *WUEi* values the treatment at the dose of 200 mg Cr^{3+} kg^{-1} soil had a reduction of 48%. For *WUE* at doses of 100 and 200 mg Cr^{3+} kg^{-1} soil there were reductions of 35% and 50%, respectively. At 15 days AAT the treatment of 100 mg Cr^{3+} kg^{-1} soil obtained a 36% and 53% increment and the dose of 200 mg Cr^{3+} kg^{-1} soil reductions of 29% and 30% for *WUEi* and *WUE*, respectively. In contrast, no significant difference ($p < 0.01$) was observed between treatments at 21 and 28 days AAT (Fig. 1D and E).

3.2. Photosynthetic pigments

A small significant difference ($p < 0.05$) was observed for the photosynthetic pigments evaluated in leaves of the CCN 51 cacao plants, submitted to different doses of Cr^{3+} in the soil (Fig. 2A and B). The content of Chl *b* and Chl (*a*+*b*) at the dose of 400 mg Cr^{3+} kg^{-1} soil, obtained reduction of 30% and 14%, respectively. While the carotenoid content and the Chl (*a*/*b*) and car/Chl (*a*+*b*) ratios, the dose of 400 mg Cr^{3+} kg^{-1} soil obtained increments of 40%, 52% and 75%, respectively. No significant differences were observed between the other treatments evaluated with the increase of Cr^{3+} doses in the soil (Fig. 2A and B).

3.3. Total Cr accumulation

The total Cr concentration in the leaves and roots of the CCN 51 cacao plants increased significantly ($p < 0.01$) at the highest doses of Cr^{3+} applied to the soil (Fig. 2C). In the leaves, the treatments with 400 and 600 mg Cr^{3+} kg^{-1} soil were significantly different from each other and higher than the doses of 100 and 200 mg Cr^{3+} kg^{-1} soil and the control. In the roots, treatments with 200, 400 and 600 mg Cr^{3+} kg^{-1} soil were significantly different from each other and higher than the dose of 100 mg Cr^{3+} kg^{-1} soil and the control. The highest accumulation of Cr, regardless of treatment, occurred in the roots. On average, 75% of the total Cr absorbed by the plants was retained in the roots and 25% was translocated to the leaves (Fig. 2C).

3.4. Ultrastructural analyses of leaf mesophyll and root

The application of Cr^{3+} in the soil caused changes in the cellular ultrastructure of the leaf mesophyll and the roots of the plants (Fig. 3). In the foliar mesophyll treatment with the dose of 600 mg Cr^{3+} kg^{-1} soil, vesicles formed with deposition of electrodense material and widely spaced thylakoids (Fig. 3D), large deposition of electrodense material in the central xylem (Fig. 3E), disorganization of thylakoid membranes with destruction of chloroplasts and deposits of electrodense material in the leaf mesophyll (Fig. 3F). In the control treatment

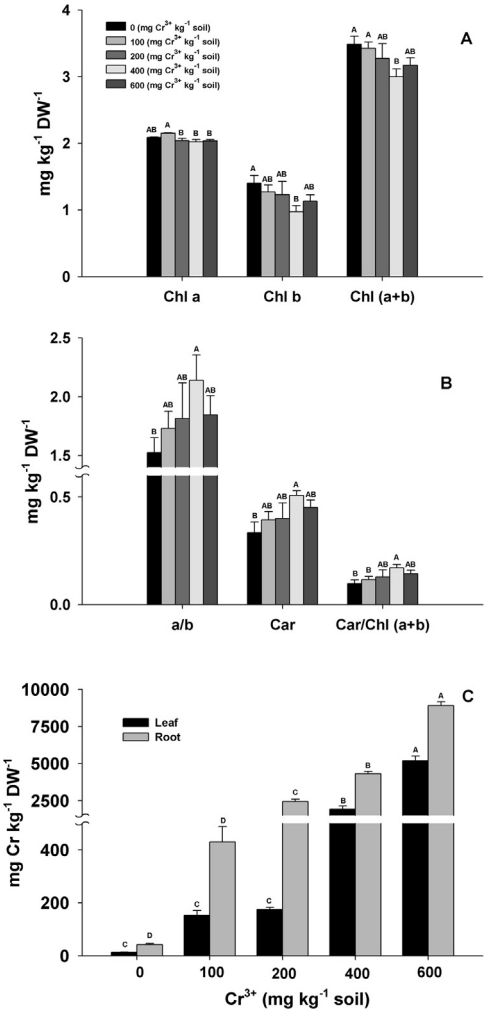

Fig. 2. Leaf photosynthetic pigment content (A and B) and total Cr accumulation (C) in the roots and leaves of CCN 51 clonal genotype plants submitted to five increasing doses of Cr^{3+} in soil. Mean values of six biological replicates ± SE for photosynthetic pigments and four biological replicates ± SE for Cr total. Capital letters indicate averages comparisons between treatments by the Tukey test ($p < 0.01$). (A and B) Determined at 96 h after application of treatments (AAT);(C) determined at 28 days AAT, except treatments of 400 and 600 mg Cr^{3+} kg^{-1} soil that were closed at 4 days AAT.

(Fig. 3A) and in the dose of 200 mg Cr^{3+} kg^{-1} soil (Fig. 3B and C), nucleus, mitochondria, chloroplasts with starch grains and cell wall were observed. In contrast, at the dose of 200 mg Cr^{3+} kg^{-1} soil, there was a large deposition of electrodense material in the cell vacuole (Fig. 3B and C). On the other hand, in the roots, the dose of 200 mg Cr^{3+} kg^{-1} soil, promoted retraction of the protoplasm (Fig. 3H), formation of vesicles, deposition of electrodense material on xylem cells (Fig. 3I) and rupture of cell walls with of the protoplasm (Fig. 3J) were observed. However, at the dose of 600 mg Cr^{3+} kg^{-1} soil, there was irreversible destruction of mitochondria (Fig. 3K), accumulation of electrodense material in the cell wall and retraction of protoplasm due to plasmolysis (Fig. 3L), when compared to the control treatment, whose cells of the root system remained intact (Fig. 3G).

3.5. Malondialdehyde (MDA)

Increases in the MDA content were observed after 12 h AAT in the treatment with 100 mg Cr^{3+} kg^{-1} soil (30%), when compared to the control. In the 24 h period AAT, the doses of 100, 200 and 600 mg Cr^{3+} kg^{-1} soil promoted increases of 13%, 21% and 15%, respectively. In the 48 h AAT period, there was a 12% increase in MDA content only at the dose of 200 mg Cr^{3+} kg^{-1} soil. On the contrary, in the 96 h AAT period, there were increases of 38%, 16% and 10% in the doses of 200, 400 and 600 mg Cr^{3+} kg^{-1} soil, respectively (Fig. 4A).

3.6. Proline

The proline content in leaves of the CCN 51 plants increased significantly ($p < 0.01$) with the time of exposure to Cr^{3+} treatments at doses of 200, 400 and 600 mg Cr^{3+} kg^{-1} soil (Fig. 4B). The highest concentrations were observed at 48 h and 96 h AAT intervals. The treatments with 200, 400 and 600 mg Cr^{3+} kg^{-1} soil increased the proline content at 19, 40 and 74 times in relation to the control at 96 h AAT (Fig. 4B).

3.7. Antioxidant metabolism

A significant increase ($p < 0.01$) in the activity of the antioxidative metabolism enzymes was observed between the treatments with Cr^{3+} applied to the soil and the exposure times to the metal (Fig. 5). Higher ascorbate peroxidase activity (APX) (Fig. 5A) was observed at the dose of 600 mg Cr^{3+} kg^{-1} soil at all evaluated intervals. This treatment promoted an increase in APX activity that varied from 198% at 3 h AAT to 526% at 96 h AAT, when compared to the control treatment. The evaluation intervals of 6 h and 96 h AAT were significantly higher than the other evaluation periods for the dose of 600 mg Cr^{3+} kg^{-1} soil. At the doses corresponding to 100, 200 and 400 mg Cr^{3+} kg^{-1} soil, the APX activity was similar to or lower than the control and there were no significant differences between the exposure times to the metal (Fig. 5A).

Higher activity of the catalase enzyme (CAT) (Fig. 5B) was observed among all treatments at 96 h AAT, whose increments ranged from 53% to 123%, when compared to the control. At 48 h AAT significantly higher activity was observed in treatments with 100, 200 and 400 mg Cr^{3+} kg^{-1} soil in increments of 52%, 28% and 33%, respectively. On the other hand, the dose of 600 mg Cr^{3+} kg^{-1} soil promoted an increase of 24% at 3 h AAT, while the dose of 100 mg Cr^{3+} kg^{-1} soil promoted a 21% increase at 24 h AAT. In the other times of metal exposure, there were reductions in CAT activity up to 32% (Fig. 5B).

For the guaiacol peroxidase activity (GPX) (Fig. 5C), a significant increase was observed in relation to the control for all doses of Cr^{3+} applied to the soil and time of exposure to the metal. At doses of 100 and 200 mg Cr^{3+} kg^{-1} soil there were greater increases in GPX activity at 3, 6 and 12 h AAT; while at doses of 400 and 600 mg Cr^{3+} kg^{-1} soil the highest increases in activity were observed at 3, 6, 12 and 48 h AAT (Fig. 4C).

There was a significant increase in glutathione reductase activity (GR), ranging from 23% at 3 h AAT to 101% at 96 h AAT, in the treatment with 100 mg Cr^{3+} kg^{-1} soil at all times of exposure to metal (Fig. 5D). In addition, at 200 mg Cr^{3+} kg^{-1} soil, GR increased at 3, 6, 24 and 96 h AAT, with increases of 24%, 89%, 84% and 164%, respectively. On the other hand, the dose of 400 mg Cr^{3+} kg^{-1} soil promoted an increase in GR activity, at 3 and 96 h AAT, of 30% and 70%, respectively, when compared to the control treatment (Fig. 5D).

Greater activity of the superoxide dismutase (SOD) (Fig. 5E) was observed in the treatment with 400 mg Cr^{3+} kg^{-1} soil in the 3, 6 and 12 h AAT intervals, increasing by 2.83%, 2.79% and 1.4%, respectively. The dose of 600 mg Cr^{3+} kg^{-1} soil promoted increases in the intervals of 3 h AAT (1.57%), 6 h AAT (1.92%), 12 h AAT (1.56%), 24 h AAT (1.61%) and 96 h AAT (1.42%). On the other hand, at the dose of 100 mg Cr^{3+} kg^{-1} soil there was greater activity of SOD (1.5%) at 6 h AAT. At the dose of 200 mg Cr^{3+} kg^{-1} soil, in the 96 h AAT interval, with an increase of 2.5%, when compared to the control (Fig. 5E).

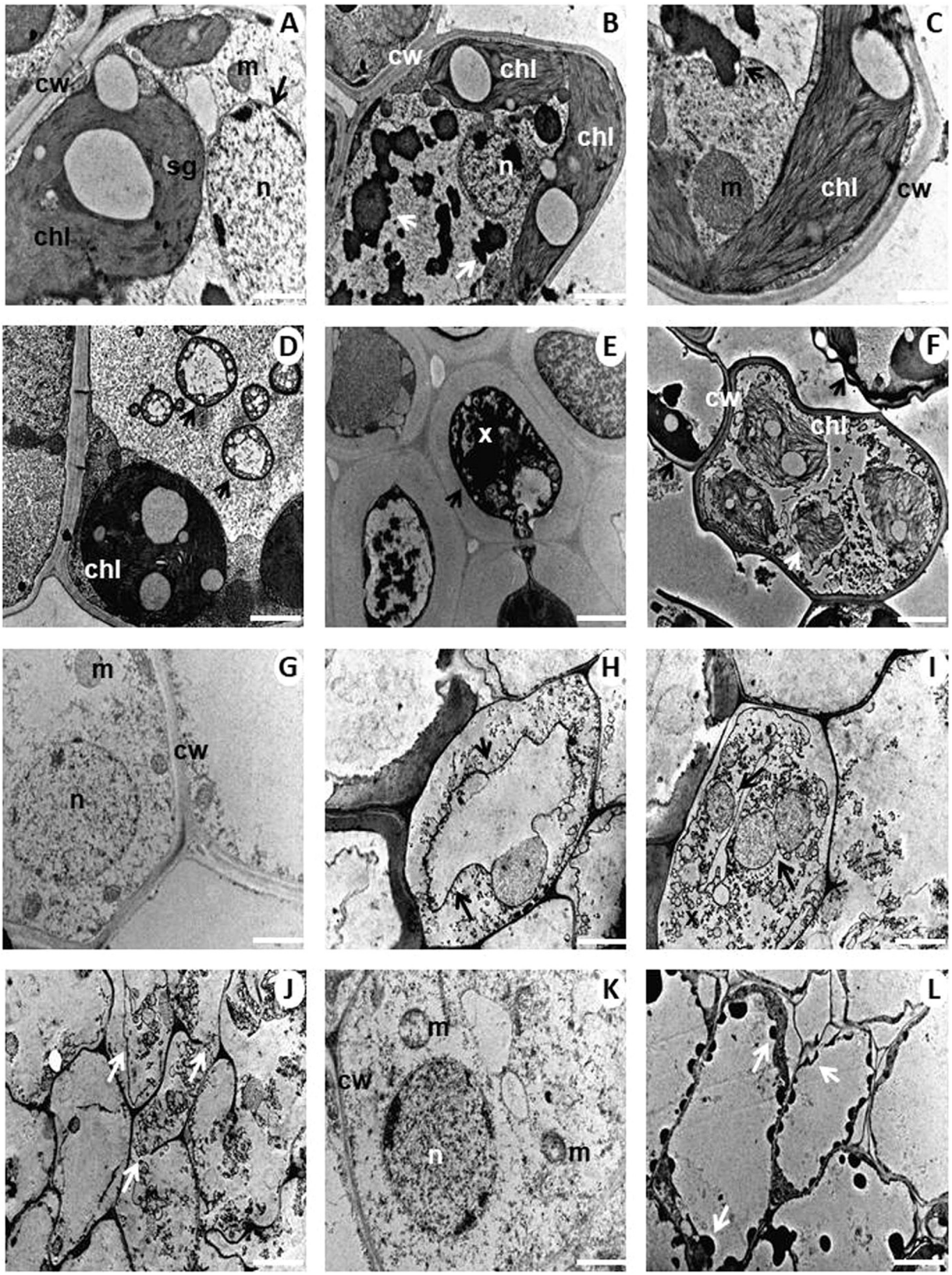

Fig. 3. Microphotographs (TEM) of transverse sections of the leaf mesophyll (A-F) and root (G-L) cross sections of plants of the clonal cacao genotype CCN 51 submitted to five increasing doses of Cr^{3+} in the soil. Leaves: control (A), 200 mg Cr^{3+} kg^{-1} soil (B and C) and 600 mg Cr^{3+} kg^{-1} soil (D, E and F). Roots: control (G), 200 mg Cr^{3+} kg^{-1} soil (H, I and J) and 600 mg Cr^{3+} kg^{-1} soil (K and L). Arrows indicate deposition of electrodense material in the vacuoles (B and C); formation of vesicles (D and I); deposition of electrodense material in the central xylem (E); disorganization of thylakoid membranes, destruction of chloroplasts and deposition of electrodense material (F); ultra-retraction of protoplasm (H); rupture of cell wall (J) and accumulation of electrodense material in the cell wall (L). n: nucleus, m: mitochondrion, cw: cell wall, chl: chloroplast, sg: starch grains, x: xylem. Bars = 1 μm (A, C, G and K), 2 μm (B, D, E, H and I) and 0.5 μm (F, J and L).

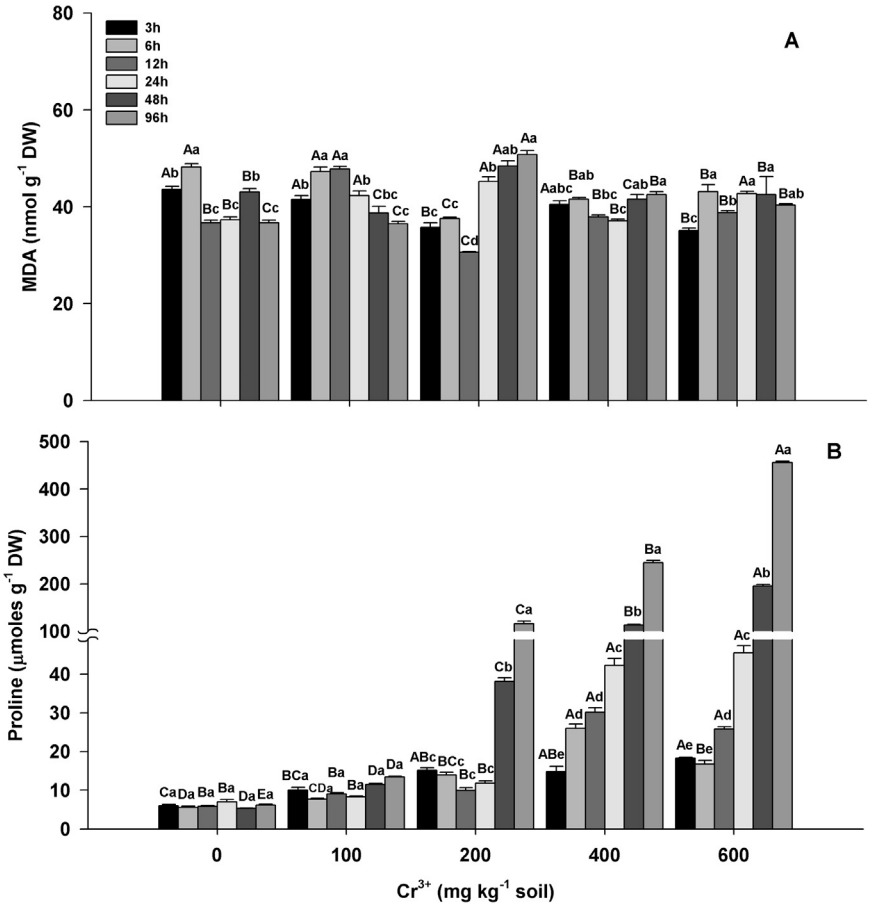

Fig. 4. (A) Concentration of malondialdehyde content (MDA) and (B) proline in leaves of plants of the cacao genotype CCN 51 submitted to five increasing doses of Cr^{3+} in the soil. Mean values of five biological replicates ± SE for MDA and four biological replicates ± SE for proline. Capital letters indicate mean comparisons between Cr^{3+} treatments in soil. Small letters indicate averages comparisons between the evaluation intervals by the Tukey test ($p < 0.01$).

3.8. Gene expression

A significant difference ($p < 0.01$) in the expression of the evaluated genes (*psbA*, *psbO*, *Mt2b*, *phyt*, *sod cyt* and *sod chl*) was observed as a function of the Cr^{3+} doses applied to the soil and the exposure time to the metal (Fig. 6). In the 24 h AAT period, the highest expressions of the *psbA*, *psbO*, *Mt2b* and *sod chl* genes (Fig. 6A, B, C and F) occurred in the treatment of 200 mg Cr^{3+} kg^{-1} soil, with increases of 254%, 394%, 204% and 1044%, respectively. However, at the dose of 100 mg Cr^{3+} kg^{-1} soil, there was an increase of 1032%, 104%, 135% and 319% in expression of the *sod chl*, *psbA*, *psbO* and *phyt* genes (Fig. 6F, A, B and D). The highest *phyt* and *sod cyt* genes expression (Fig. 6D and E) were observed at doses of 400 and 600 mg Cr^{3+} kg^{-1} soil, with increments of 1466% and 571%, respectively. In addition, doses of 400 and 600 mg Cr^{3+} kg^{-1} soil also promoted expression of *psbA* (139% and 62%) and *psbO* (237% and 56%), (Fig. 6A and B) respectively. On the other hand, treatments with 400 and 600 mg Cr^{3+} kg^{-1} soil repressed *Mt2b* gene expression (Fig. 6C) in 82% and 40%, respectively. A significant increase of 407% and 565% were also observed in *phyt* gene expression (Fig. 6D), in treatments with 200 and 600 mg Cr^{3+} kg^{-1} soil, respectively.

At the 96 h AAT exposure time, the highest expressions of *psbA*, *phyt* and *sod cyt* genes (Fig. 6A, D and E) were observed in the treatment with 600 mg Cr^{3+} kg^{-1} soil, with increases of 73%, 638% and 1357%, respectively. In addition, the dose of 600 mg Cr^{3+} kg^{-1} soil promoted a 63% increase in *Mt2b* expression (Fig. 6C). On the other hand, the dose of 100 mg Cr^{3+} kg^{-1} soil promoted an increase in the expression of the *psbO*, *Mt2b* and *phyt* genes (Fig. 6B, C and D) of 245%, 253% and 371%, respectively. The treatment with 200 mg Cr^{3+} kg^{-1} soil promoted increases of 58% in *psbA* gene expression, 212% in *psbO* and 484% in *phyt* expression (Fig. 6A, B and D). In contrast, the treatment with 400 mg Cr^{3+} kg^{-1} soil promoted increases of 102%, 318% and 292% in expression of the *Mt2b*, *sod chl* and *sod cyt* genes (Fig. 6), respectively.

4. Discussion

Leaf gaseous exchanges (P_N, *gs* and *E)* in the CCN 51 cacao clonal cultivar were severely affected by Cr^{3+} treatments at doses of 200, 400 and 600 mg Cr^{3+} kg^{-1} soil, 1 day AAT (Fig. 1), due to damage caused in the photosynthetic apparatus and changes influenced in the stomata mainly by the increase of Cr^{3+} in leaf at higher doses of applied Cr and the time of exposure to the metal. These changes can be explained by several factors such as ultrastructural damage in the chloroplast, decrease of CO_2 fixation due to reduction of *gs* and decrease of expression of genes like *psbA* and *psbO*, besides changes in enzymatic activity and MDA content (Panda and Choudhury, 2005; Shahid et al., 2017). Severe changes in leaf gas exchange have also been reported for the macrophytes *Alternanthera philoxeroides*, *Borreria scabiosoides*, *Polygonum ferrugineum* and *Eichhornia crassipes* (Mangabeira et al., 2011), for *Genipa americana* (Santana et al., 2012) subjected to Cr^{3+} stress in nutrient solution.

The recovery of photosynthetic activity at the dose of 200 mg Cr^{3+} kg^{-1} soil, at 4 days AAT (Fig. 1A), can be explained in part by the maintenance of the photosynthetic pigment contents (Fig. 2), and by the increase of the expression of the *psbA* (Fig. 6A) in the 24 h AAT, and *psbO* genes (Fig. 6B) in the 24 h and 96 h AAT intervals. The function of photosynthetic pigments is to absorb light energy and transferring it to electrons (Taiz et al., 2017). The *psbA* gene is responsible for electron transfer during photosynthetic activity. However, the *psbO* gene is responsible for the proper functioning of the oxygen evolution complex (Cheng et al., 2016) during the oxidation process of the water molecule. Variations in *psbO* concentration, directly influences photosynthesis and plant growth (Rehem et al., 2011a, 2011b). Studies with plants of *T. cacao* subjected to Cd toxicity have shown that the repression of *psbO*

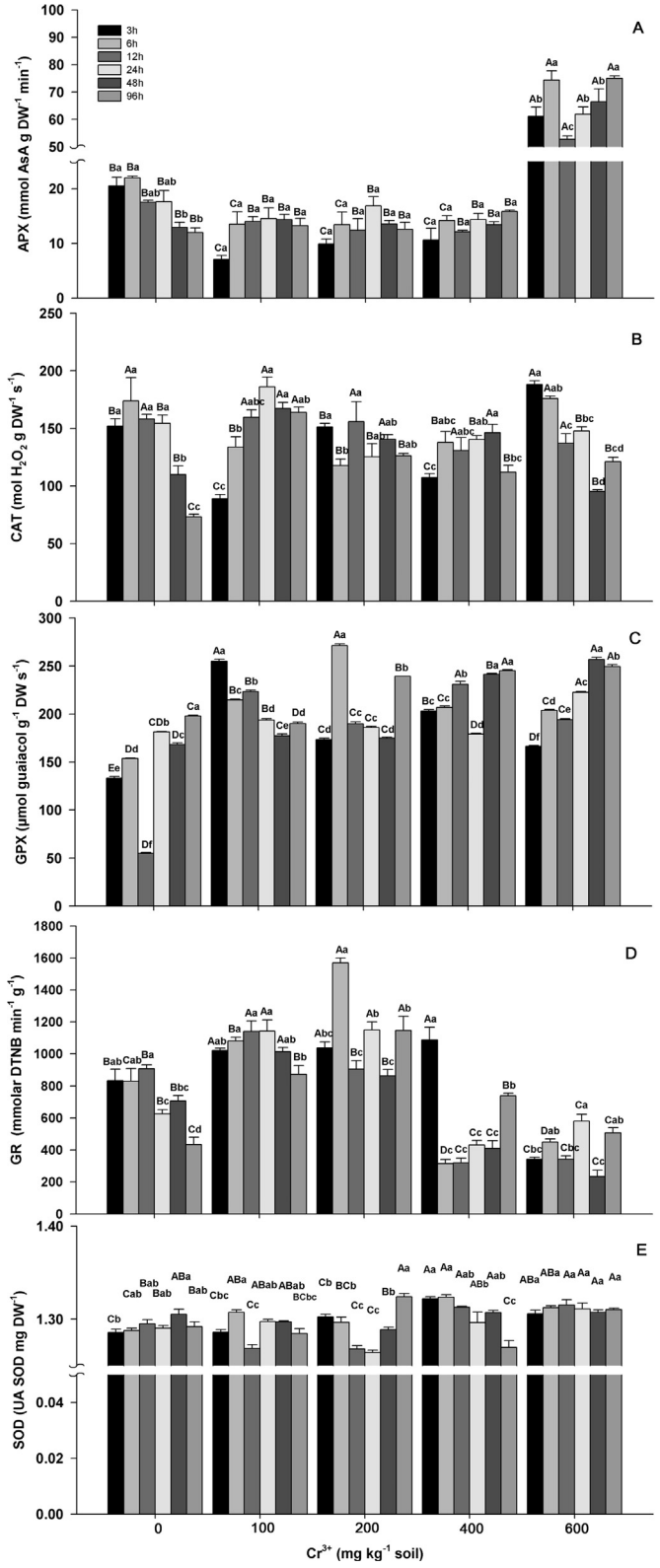

Fig. 5. Activity of the enzymes of the antioxidative metabolism. (A) APX - ascorbate peroxidase, (B) CAT - catalase, (C) GPX - guaiacol peroxidase, (D) GR - glutathione reductase and (E) SOD - dismutase superoxide in plant leaves of the clonal genotype of cacao CCN 51 submitted to five increasing doses of Cr^{3+} in the soil. Mean values of four biological replicates ± SE. Capital letters indicate mean comparisons between Cr^{3+} treatments in soil. Small letters indicate mean comparisons between the evaluation intervals by the Tuckey test ($p < 0.01$).

expression is a mechanism to protect protein D1, as a function of oxidative stress mediated by ROS, preventing damage to PS2 (Araújo et al., 2017). Thus, greater expressions of *psbA* and *psbO* genes (Fig. 6A and B) ensure the maintenance of PS2 functions.

The highest activity of the foliar gas exchange at the dose of 100 mg Cr^{3+} kg^{-1} soil (Fig. 1A, B and C) can be explained by the biphasic dose-response process called hormesis (Poschenrieder et al., 2013; Shahid et al., 2017). Chromium, applied at low doses, can induce positive hormonal effects, depending on the plant species and the valence in which it occurs, but at high doses it is phytotoxic (Shahid et al., 2017). Some studies have reported the occurrence of beneficial events in the application of low doses of Cr^{3+} in plants, such as increased carbon assimilation in *Eichhornia crassipes* (Paiva et al., 2009), stimulation of root growth in *Allium cepa* bulbs (Patnaik et al., 2013), increased essential oil production and fresh biomass of shoot and root in *Mentha citrata* (Prasad et al., 2010) and increased dry biomass of roots and shoot of *Solanum nigrum* (UdDin et al., 2015). Thus, the increase in photosynthetic activity at the dose of 100 mg Cr^{3+} kg^{-1} soil (Fig. 1A, B and C) may be due to a hormesis effect, along with maintenance of chloroplastidic pigment contents (Fig. 2A and B), and to the increase in expression of the *psbA* genes (Fig. 6A), in the 24 h period AAT, and *psbO* (Fig. 6B) in the period of 24 and 96 h AAT.

The intrinsic (*WUEi*) (Fig. 1D) and instantaneous (*WUE*) (Fig. 1E) water use efficiencies were significantly ($p < 0.01$) affected as a function of the increase in Cr^{3+} concentration in the soil and the time of exposure to metal. Such changes indicate that treatments with Cr^{3+} interfered in the ability of the leaves to regulate the loss of water via *gs* and *E* associated to P_N. When P_N and *gs* vary proportionally and linearly, *WUE*i and *WUE* decrease with the reduction of *gs*, causing a reduction in photosynthetic efficiency during the stress event (Taiz et al., 2017). *WUE* has greater environmental influence because *E* is dependent on stomatal opening and vapor pressure deficit (DPV) in the leaf boundary air layer. While *WUE*i depends only on the stomatal opening excluding the environmental effect, ie the evaporative demand on the water flows out of the leaf (Fischer and Turner, 1978).

Alterations of chloroplastidic pigments in plants submitted to stress by Cr^{3+} has been reported in the literature for some species such as *Brassica napus* (Afshan et al., 2015), *Hibiscus cannabinus* (Ding et al., 2016) and *Chenopodium quinoa* (Scoccianti et al., 2016). In our study, we observed small significant changes in chloroplastidic pigment levels in the treatment with 400 mg Cr^{3+} kg^{-1} soil (Fig. 2). The decrease in *Chl* levels can be explained by the inhibition of enzymes involved in chlorophyll biosynthesis, confirming that cocoa plants are more intolerant to Cr^{3+} stress. While the increase in carotenoid content may be related to its antioxidant function in the inactivation of reactive oxygen species (ROS) (Taiz et al., 2017) under stress conditions. Similar results have been reported in *Chenopodium quinoa* (Scoccianti et al., 2016).

The highest concentrations of total Cr were detected in the roots (Fig. 2C). On average, the roots of the cocoa plants accumulated 75% of total Cr absorbed by the plants, demonstrating root efficiency in the retention of absorbed Cr, preventing its translocation to the leaves. Our results are in agreement with the study of Ding et al. (2016) whose concentration of Cr in the roots of *Hibiscus cannabinus* was 30 times higher than in the aerial part and with the study of López-Luna et al. (2009), which verified high levels of Cr in the roots of *Sorghum* dependent on the increase of concentrations of Cr^{3+} in the soil.

Excessive Cr accumulation in the roots has been evaluated as an exclusion response of the tolerant plants, with the objective of avoiding their transport to the aerial part (Caldelas et al., 2012). Alterations related to the accumulation of electrodense material as a function of Cr have been considered by many researchers as a mechanism of detoxification or even tolerance developed by plants (Shahid et al., 2017; Singh et al., 2013). Restriction in the absorption by immobilization of the metal in the cell wall of the roots, reduction of plasma membrane translocation, complexation of the metal with organic acids and amino acids and chelation with peptides (metallothioneins and

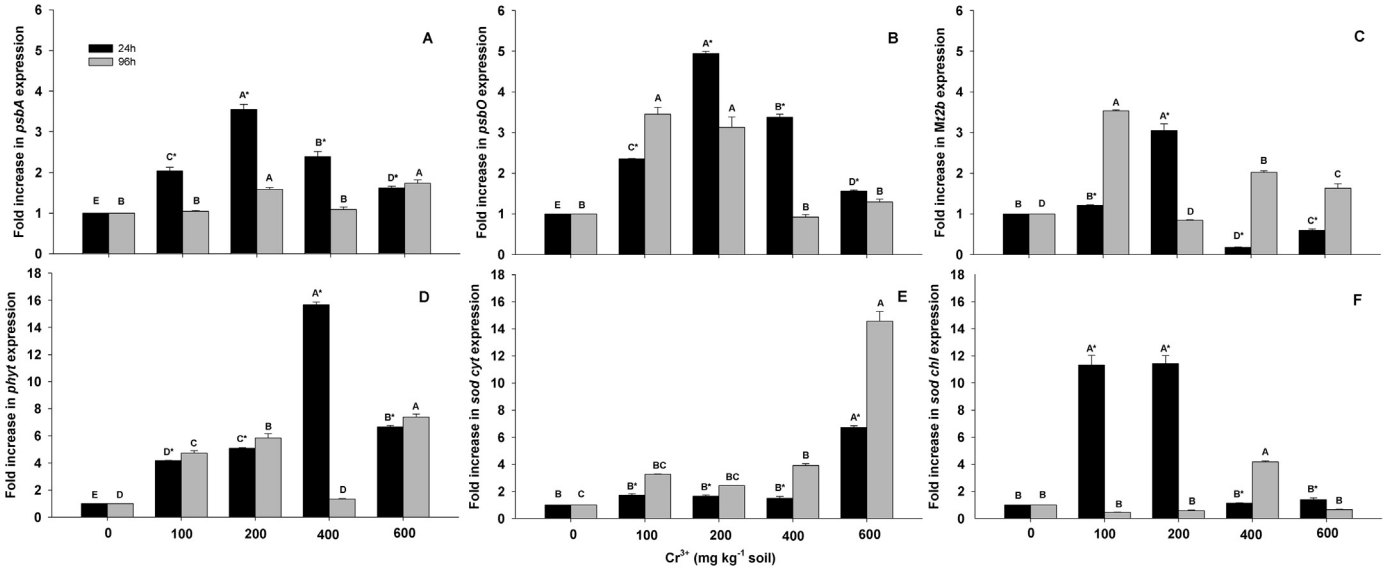

Fig. 6. Relative expression of genes coding for protein biosynthesis *psbA* (A), *psbO* (B), metallothioneins - *Mt2b* (C), phytochelatins - *phyt* (D), cytoplasmic superoxide dismutase - *sod cyt* (E), and chloroplast superoxide dismutase - *sod chl* (F) in plant leaves of the clonal CCN 51 cocoa genotype subjected to five increasing doses of Cr^{3+} in soil. Mean values of three biological replicates and two technical replicates ± SE. Capital letters indicate mean comparisons between treatments of Cr^{3+} in the soil by the Tukey test ($p < 0.01$). Statistical significance among the evaluated intervals was determined by ANOVA, followed by the *t*-test (* $p < 0.01$).

phytochelatins) in the roots and leaf vacuoles are part of this mechanism (Gomes et al., 2017). In our work, this mechanism can be observed in cocoa plants submitted to doses of 200 and 600 mg Cr^{3+} kg^{-1} soil, with accumulation of electrodense material in the root vacuoles, very close to the cell wall (Fig. 3H and L). It was also observed that an accumulation of electrodense material in the xylem of the roots and leaves, corroborating with the findings described in the literature, demonstrating that Cr, after absorption by the root system, is transported to the aerial part of the plants via xylem (Hayat et al., 2012).

The presence of vesicular bodies in the leaf vacuoles (Fig. 3D) and root xylem (Fig. 3I) may also be related to a detoxification mechanism, called macroautophagia, being this, the best explored type of autophagy in plants (Taiz et al., 2017). Autophagy is considered a sophisticated mechanism for the recycling of damaged or unwanted intracellular constituents (Li and Vierstra, 2012). Induction of autophagy due to heavy metal stress were reported in plants of *Theobroma cacao* subjected to Cd (Araujo et al., 2017) and *Lespedeza chinensis* and *Lespedeza davidii* treated with Pb (Zheng et al., 2012).

Another important mechanism developed by plants for detoxification and tolerance to heavy metals is the chelation of metals by high-affinity ligands such as phytochelatins (*phyt*) and metallothioneins (*Mt2b*) (Srivastava et al., 2017). The increase of the *phyt* expression with the increase of the dose of Cr^{3+} in the soil (Fig. 6D) and *Mt2b* (Fig. 6C) contributes to the reduction of metal concentration in the cytosol by Cr^{3+} sequestration, inactivating the metal in the cytoplasm and compartmentalizing the Cr-protein complex in the vacuoles (Hasan et al., 2017). *phyt* biosynthesis is rapidly activated in the presence of heavy metals, using reduced glutathione (GSH) as the substrate. Similar phytochelatins induction results were obtained by Diwan et al. (2010), when evaluating plants of *Vigna radiata* and *Brassica juncea* submitted to Cr stress. On the other hand, the increase in *Mt2b* expression was greater at the 96 h AAT exposure time, except for the dose 200 mg Cr^{3+} kg^{-1} soil, which occurred 24 h AAT (Fig. 6C). Metallothioneins are induced in the presence of heavy metals and are involved in the homeostasis of essential and toxic elements present in excess in plants. Studies with *Theobroma cacao* plants submitted to Cu toxicity showed that the induction of the expression of *Mt2b* at 12 h AAT, may be a protective tolerance strategy to accumulate a higher Cu content in the roots, aiming to maintain the metabolic process in the leaves (Souza et al., 2014). Increased expression of *phyt* and *Mt2b* in cocoa plants subjected to heavy-metal stress has been reported by several authors (Araujo et al., 2017; Castro et al., 2015; Reis et al., 2015; Souza et al., 2014).

Disorganization of thylakoid membranes with destruction of chloroplasts, widely spaced thylakoids, plasmolysis, rupture of cell walls and destruction of mitochondria in the roots are related to the oxidative stress promoted by excess of ROS (Fig. 3). The increase of ROS induced by Cr is an important mechanism that may contribute to the observed changes in the photosynthetic activity, since they damage polyunsaturated fatty acids and structural proteins (Rodriguez et al., 2011). In addition, excessive accumulation of ROS may alter cellular homeostasis causing various cell lesions that can lead to programmed cell death and autophagy (Hasan et al., 2017). The irreversible chloroplast damages of the cocoa plants subjected to a higher dose of Cr^{3+} (600 mg Cr^{3+} kg^{-1} soil) may be responsible for the severe reduction of foliar gas exchange due to the low recovery of P_N at 4 days AAT. Similar ultrastructural results have also been reported in other species subjected to Cr^{3+} (Mangabeira et al., 2011), as well as in cocoa plants subjected to Al, Cd, Pb and Cu (Almeida et al., 2015, Araujo et al., 2017, Castro et al., 2015, Souza et al., 2014).

CCN 51 plants exposed to Cr^{3+} toxicity in the soil, triggered not only alterations in physiological processes, but also significant changes in MDA content of cell membranes (Fig. 4), induced by the increase of reactive oxygen species (ROS). Our findings differed from other results found in the literature, where the higher concentrations of Cr provide higher levels of MDA (Afshan et al., 2015; Anjum et al., 2017). In *T. cacao*, higher peaks of MDA were observed in treatments with 100 and 200 mg Cr^{3+} kg^{-1} soil and exposure times of 12 and 24 h AAT and 24, 48 and 96 h AAT, respectively. On the other hand, the treatments with higher doses had little alteration in the contents of MDA when compared to the control (Fig. 4). These results may be explained by changes in the activity of the antioxidative enzymes (Afshan et al., 2015; Anjum et al., 2017). The lower activity of the SOD, APX and CAT (Fig. 5) enzymes were observed in the same exposure times to treatments of 100 and 200 mg Cr^{3+} kg^{-1} soil. On the other hand, in the treatments with higher doses of Cr^{3+} in the soil, greater activities of the SOD, APX, GPX and CAT enzymes (Fig. 5) corresponded to lower levels of MDA (Fig. 4). Thus, we can deduce that higher concentrations of MDA, as indicative of the maintenance of oxidative stress (Dey et al., 2007), are related to lower enzymatic activity in plants of the clonal cacao genotype CCN 51.

Antioxidant enzymes present as the main line of defense against ROS, work in synchrony to eliminate them (Choudhury et al., 2013; Shahid et al., 2017). In addition, plants with higher enzymatic activity are more tolerant to different types of stress. In our findings, higher SOD activity was observed (Fig. 4E) in the treatments with the highest concentrations of Cr^{3+} in the soil, demonstrating a rapid activation of defense mechanisms in practically all exposure times evaluated. SOD found in almost all cellular compartments, is the first antioxidant enzyme to act against ROS-mediated oxidative stress (Taiz et al., 2017).

At lower doses of Cr^{3+} in the soil, low activation of SOD (Fig. 4E) was observed in the leaves at the evaluated exposure times, thus maintaining the balance between generation and removal of ROS (Shahid et al., 2017). However, greater activation of GPX (Fig. 5C) was observed in the three initial times of exposure evaluated and CAT (Fig. 5B) at the three final exposure times, whereas APX (Fig. 5A) was not activated at low dosages of Cr^{3+} in soil. The activity of some antioxidant enzymes can be suppressed when plants are subjected to an abiotic stress, and when this occurs, positive induction of other enzymes becomes essential in order to maintain redox homeostasis in plants (Choudhury et al., 2013; Vaahtera et al., 2014).

In our study, we observed that there was a synchronized action of the antioxidant enzymes evaluated, aiming to limit oxidative stress in cocoa plants, and that peroxidases were more efficient in H_2O_2 detoxification in the presence of high concentration of Cr^{3+} in the soil. At higher doses of Cr^{3+} in the soil, greater activation of GPX (Fig. 5C) occurred at all evaluated exposure times, whereas for CAT (Fig. 5B) it occurred in the last two exposure times, whereas APX activation (Fig. 5A) occurred only at the highest Cr^{3+} dose at all exposure times evaluated. The increase in APX and GPX activity may be related to the reduction of foliar gas exchange in the treatments with higher doses of Cr^{3+} in the soil. Its increase may indicate the physiological state of plants, since ROS are by-products of photosynthesis and respiration, produced in chloroplasts and mitochondria, respectively (Mittler, 2017). Increased SOD activity, induced by Cr^{3+} stress, has been reported in *Parthenium hysterophorus* (UdDin et al., 2015) and *Zea mays* (Anjum et al., 2017). Similar results for CAT, APX and GPX were found in *Salvinia natans* (Dhir et al., 2009). In *Theobroma cacao*, increased activation of SOD and GPX when plants were submitted to Cd stress (Araujo et al., 2017) and GPX activation in leaves and roots by Pb (Reis et al., 2015) were reported.

Glutathione reductase (GR) (Fig. 5D) is one of the antioxidant enzymes that have the function of regulating the redox state of cells (Choudhury et al., 2013). GR participates in the maintenance reactions of the reduced glutathione levels (GSH) (Foyer and Noctor, 2011), with the chloroplasts being the place of its greater activity (Pandey et al., 2009). Higher concentrations of GR in the treatments with the lowest doses of Cr^{3+} in the soil (Fig. 5D), indicate the occurrence of redox balance maintenance, as a way of reducing and protecting cocoa plants from oxidative stress. On the other hand, the lower activity of GR in high concentration of Cr^{3+} in the soil indicates that there was alteration in redox homeostasis in these treatments. Similar results were reported by Pandey et al. (2009).

In addition to the antioxidant enzymes, the accumulation of amino acids such as proline has been well reported in the literature in the fight against oxidative stress promoted by heavy metals, including Cr (Anjum et al., 2017; Dey and Mondal, 2016, UdDin et al., 2015). In our study, proline levels were higher at higher doses of Cr^{3+} in the soil during and after 48 h exposure to the metal (Fig. 4). In addition, the increase in proline content coincided with increased activity of GPX peroxidases (Fig. 5C) and APX (Fig. 5A). The results of our work agree with the results reported in *Solanum nigrum*, where this correspondence was also found in high doses of Cr^{3+} in soil (UdDin et al., 2015). According to Mourato et al. (2012), high levels of proline, under abiotic stress, can increase the resistance of plants to the stress factor, activating antioxidant enzymes, participating in the maintenance of redox homeostasis and eliminating ROS (Mittler, 2017).

Studies suggest that ROS act as biological indicators in the regulation of stress (Hossain et al., 2012), triggering the expression of several genes that encode proteins involved in the production, perception and elimination of ROS in cells (Mittler, 2017; Vaahtera et al., 2014). The increase in the expression of *sod Cyt* (Fig. 6E), at doses of 200, 400 and 600 mg Cr^{3+} kg^{-1} soil, coincided with the increase in the activity of the main enzymes of the antioxidative system (Fig. 5), and with the increase of the proline content (Fig. 4B). Increased expression of genes encoding antioxidant enzymes contributes to the maintenance of the activity of antioxidant compounds, aiming for the elimination of ROS and reinforcing the antioxidant defense system. In addition, the immediate elimination of ROS, due to increased oxidative stress, occurs preferentially at its production sites, by the activation of antioxidant substances present at this site (Hossain et al., 2012). The accumulation of higher proline levels (Hayat et al., 2012) and the activation of APX, GPX, CAT (Mittler, 2017) and SOD (Choudhury et al., 2013) also occur in the cytoplasm, supporting the theory previously discussed that there was a synchronized action to eliminate ROS. Increased expression of *sod Cyt* in cocoa leaves has been reported in the highest doses of Al^{3+}, Cd, Pb, and Cu (Almeida et al., 2015, Araujo et al., 2017, Castro et al., 2015; Reis et al., 2015; Souza et al., 2014). On the other hand, increases in the expression of *sod Chl* (Fig. 6F), were observed at doses of 100 and 200 mg Cr^{3+} kg^{-1} soil, 24 h AAT, coinciding with increases in the activation of SOD in the treatment with 100 mg Cr^{3+} kg^{-1} soil, and at 96 h AAT in the treatment 200 mg Cr^{3+} kg^{-1} soil. Given the previously discussed hypothesis that in the lower doses of Cr^{3+} in soil occur maintenance of the balance between generation and removal of ROS (Shahid et al., 2017), since ROS act as signaling genes for the induction of biosynthesis of antioxidant enzymes.

5. Conclusions

The tolerance of the CCN 51 clonal plants to Cr^{3+} toxicity depends on its concentration in plant and time of its exposure to this metal. Among the tested doses, 100 mg Cr^{3+} kg^{-1} soil showed the best performance under metal stress condition, operating a prompt, multiple response at enzymatic, molecular and physiological levels. Doses of Cr^{3+} equal to or greater than 200 mg Cr^{3+} kg^{-1} soil appear to be very toxic, remarkably interfering with the overall metabolism of this species. High content of Cr in soil promoted serious ultrastructural changes, which can lead to death. All alterations observed in *T. cacao* plants subjected to increasing levels of Cr^{3+} suggest that plants grown in soils with high levels of Cr can be negatively affected in their growth and metabolism. As a strategy for tolerance to Cr^{3+} toxicity in the soil, cacao retained on an average 75% of the total Cr absorbed in the roots indicating a low mobility within the plant. These results also indicate Cr is more relevant to phytotoxicity than to food safety risk assessments, since the addition of Cr to soil promoted physiological and the ultrastructural changes in plants of *T. cacao*."

Acknowledgements

The second author gratefully acknowledges Brazil's National Council for Scientific and Technological Development (CNPq), Brazil, for the concession of a fellowship of scientific productivity. Junea Leandro do Nascimento was supported by CAPES (Coordination of Superior Level Staff Improvement). We thank Dr. M. Elson for excellent review of this paper.

Appendix A. Supplementary material

Supplementary data associated with this article can be found in the online version at http://dx.doi.org/10.1016/j.ecoenv.2018.04.058.

References

Abbott, W.S., 1925. A method of computing the effectiveness of on insecticide. J. Econ. Entomol. 18, 265–267. http://dx.doi.org/10.1093/jee/18.2.265a.

Afshan, S., Ali, S., Bharwana, S.A., Rizwan, M., Farid, M., Abbas, F., Ibrahim, M., Mehmood, M.A., Abbasi, G.H., 2015. Citric acid enhances the phytoextraction of chromium, plant growth, and photosynthesis by alleviating the oxidative damages in *Brassica napus* L. Environ. Sci. Pollut. Res. Int. 22, 11679–11689. http://dx.doi.org/10.1007/s11356-015-4396-8.

Almeida, A.-A.F., Valle, R.R., 2009. Cacao: ecophysiology of growth and production. In: DaMatta, F.M. (Ed.), Ecophysiology of Tropical Tree Crops. Nova Science Publishers Inc, Hauppauge, Andersen, pp. 37–70.

Almeida, A.-A.F., Gomes, F.P., Araujo, R.P., Santos, R.C., Valle, R.R., 2014. Leaf gas exchange in species of the Theobroma genus. Photosynthetica 52, 16–21. http://dx.doi.org/10.1007/s11099-013-0048-8.

Almeida, N.M., Almeida, A.-A.F., Mangabeira, P.A.O., Ahnert, D., Reis, G.S.M., Castro, A.V., 2015. Molecular, biochemical, morphological and ultrastructural responses of cacao seedlings to aluminum (Al^{3+}) toxicity. Acta Physiol. Plant 37, 5. http://dx.doi.org/10.1007/s11738-014-1732-4.

Anjum, S.A., Ashraf, U., Khan, I., Tanveer, M., Shahid, M., Shakoor, A., Wang, L., 2017. Phyto-toxicity of chromium in maize: oxidative damage, osmolyte accumulation, anti-oxidative defense and chromium uptake. Pedosphere 27, 262–273. http://dx.doi.org/10.1016/S1002-0160(17)60315-1.

Araújo, R.P., Almeida, A.-A.F., Pereira, L.S., Mangabeira, P.A.O., Souza, J.O., Pirovani, C.P., Ahnert, D., Baligar, V.C., 2017. Photosynthetic, antioxidative, molecular and ultrastructural responses of young cacao plants to Cd toxicity in the soil. Ecotoxicol. Environ. Saf. 144, 148–157. http://dx.doi.org/10.1016/j.ecoenv.2017.06.006.

Arévalo-Gardini, E., Arévalo-Hernández, C.O., Baligar, V.C., He, Z.L., 2017. Heavy metal accumulation in leaves and beans of cacao (*Theobroma cacao* L.) in major cacao growing regions in Peru. Sci. Total Environ. 605, 792–800. http://dx.doi.org/10.1016/j.scitotenv.2017.06.122.

Ashraf, A., Bibi, I., Niazi, N.K., Ok, Y.S., Murtaza, G., Shahid, M., Kunhikrishnan, A., Mahmood, T., 2017. Chromium(VI) sorption efficiency of acid-activated banana peel over organo-montmorillonite in aqueous solutions. Int. J. Phytoremediat. 19, 605–613. http://dx.doi.org/10.1080/15226514.2016.1256372.

Aslam, M., Saeed, M.S., Sattar, S., Sajad, S., Sajjad, M., Adnan, M., Iqbal, M., Sharif, M.T., 2017. Specific role of proline against heavy metals toxicity in plants. Int. J. Pure Appl. Biosci. 5, 27–34. http://dx.doi.org/10.18782/2320-7051.6032.

Bates, I.S., Waldern, R.P., Teare, I.D., 1973. Rapid determination of free proline for water stress studies. Plant Soil 39, 205–207. http://dx.doi.org/10.1007/BF00018060.

Bertoldi, D., Barbero, A., Camin, F., Caligiani, A., Larcher, R., 2016. Multielemental fingerprinting and geographic traceability of *Theobroma cacao* beans and cocoa products. Food Control. 65, 46–53. http://dx.doi.org/10.1016/j.foodcont.2016.01.013.

Boza, E.J., Motamayor, J.C., Amores, F.M., Cedeño-Amador, S., Tondo, C.L., Livingstone III, D.S., Schnell, R.J., Gutiérrez, O.A., 2014. Genetic characterization of the cacao cultivar CCN 51: its impact and significance on global cacao improvement an production. J. Am. Soc. Hort. Sci. 139, 219–229. ⟨http://journal.ashspublications.org/content/139/2/219.full⟩.

Cakmak, I., Horst, W.J., 1991. Effect of aluminum on lipid peroxidation, superoxide dismutase, catalase and peroxidase activities in root tips of soybean (*Glycine max*). Physiol. Plant 83, 463–468. http://dx.doi.org/10.1111/j.1399-3054.1991.tb00121.x.

Calabrese, E.J., 2015. Hormesis within a mechanistic context. Homeopathy 104, 90–96. http://dx.doi.org/10.1016/j.homp.2015.01.002.

Calabrese, E.J., Blain, R.B., 2009. Hormesis and plant biology. Environ. Pollut. 157, 42–48. http://dx.doi.org/10.1016/j.envpol.2008.07.028.

Caldelas, C., Bort, J., Febrero, A., 2012. Ultrastructure and subcellular distribution of Cr in *Iris pseudacorus* L. using TEM and X-ray microanalysis. Cell Biol. Toxicol. 28, 57–68. http://dx.doi.org/10.1007/s10565-011-9205-7.

Carlberg, C., Mannervik, B., 1985. Glutathione reductase. Methods Enzymol. 113, 488–495. http://dx.doi.org/10.1016/S0076-6879(85)13062-4.

Castro, A.V., Almeida, A.-A.F., Pirovani, C.P., Reis, G.S.M., Almeida, N.M., Mangabeira, P.A.O., 2015. Morphological, biochemical, molecular and ultrastructural changes induced by Cd toxicity in seedlings of *Theobroma cacao* L. Ecotoxicol. Environ. Saf. 115, 174–186. http://dx.doi.org/10.1016/j.ecoenv.2015.02.003.

Cheng, D.-D., Zhang, Z.-S., Sun, X.-B., Zhao, M., Sun, G.-Y., Chow, W.S., 2016. Photoinhibition and photoinhibition-like damage to the photosynthetic apparatus in tobacco leaves induced by *Pseudômonas syringae pv. Tabaci* under light and dark conditions. BMC Plant Biol. 16, 29. http://dx.doi.org/10.1186/s12870-016-0723-6.

Choudhury, S., Panda, P., Sahoo, L., Panda, S.K., 2013. Reactive oxygen species signaling in plants under abiotic stress. Plant Signal. Behav. 8, 23681. http://dx.doi.org/10.4161/psb.23681.

Dey, S.K., Dey, J., Patra, S., Pothal, D., 2007. Changes in the antioxidative enzyme activities and lipid peroxidation in wheat seedlings exposed to cádmium and lead stress. Braz. J. Plant Physiol. 19, 1. http://dx.doi.org/10.1590/S1677-04202007000100006.

Dey, U., Mondal, N.K., 2016. Ultrastructural deformation of plant cell under heavy metal stress in Gram seedlings. Cogent Environ. Sci. 2, 1196472. http://dx.doi.org/10.1080/23311843.2016.1196472.

Dhir, B., Sharmila, P., Saradhi, P.P., Nasim, S.A., 2009. Physiological and antioxidant responses of *Salvinia natans* exposed to chromium-rich wastewater. Ecotoxicol. Environ. Saf. 72, 1790–1797. http://dx.doi.org/10.1016/j.ecoenv.2009.03.015.

Ding, H., Wang, G., Lou, L., Lv, J., 2016. Physiological responses and tolerance of kenaf (*Hibiscus cannabinus* L.) exposed to chromium. Ecotoxicol. Environ. Saf. 133, 509–518. http://dx.doi.org/10.1016/j.ecoenv.2016.08.007.

Diwan, H., Khan, I., Ahmad, A., Iqbal, M., 2010. Induction of phytochelatins and antioxidant defence system in Brassica juncea and Vigna radiata in response to chromium treatments. Plant Growth Regul. 61, 97. http://dx.doi.org/10.1007/s10725-010-9454-0.

Farah, M.A., Ali, M.A., Chen, S.M., Li, Y., Al-Hemaid, F.M., Abou-Tarboush, F.M., Al-Anazi, K.M., Lee, J., 2016. Silver nanoparticles synthesized from *Adenium obesum* leaf extract induced DNA damage, apoptosis and autophagy via generation of reactive oxygen species. Colloids Surf. B Biointerfaces 141, 158–169. http://dx.doi.org/10.1016/j.colsurfb.2016.01.027.

Fischer, R.A., Turner, N.C., 1978. Plant productivity in arid and semiarid zones. Ann. Rev. Plant Physiol. 29, 277–317. http://dx.doi.org/10.1146/annurev.pp.29.060178.001425.

Foyer, C.H., Noctor, G., 2011. Ascorbate and glutathione: the heart of the redox hub. Plant Physiol. 155, 2–18. http://dx.doi.org/10.1104/pp.110.167569.

Giannopolitis, C.N., Ries, S.K., 1977. Superoxide dismutases I. Occurrence in higher plants. Plant Physiol. 59, 309–314. http://dx.doi.org/10.1104/pp.59.2.309.

Gomes, M.A.C., Hauser-Davis, R.A., Suzuki, M.S., Vitória, A.P., 2017. Plant chromium uptake and transport, physiological effects and recent advances in molecular investigations. Ecotoxicol. Environ. Saf. 140, 55–64. http://dx.doi.org/10.1016/j.ecoenv.2017.01.042.

Han, F.X., Su, Y., Sridhar, B.B.M., Monts, D.L., 2004. Distribution, transformation and bioavailability of trivalent and hexavalent chromium in contaminated soil. Plant Soil. 265, 243. http://dx.doi.org/10.1007/s11104-005-0975-7.

Hasan, M.K., Cheng, Y., Kanwar, M.K., Chu, X.-Y., Ahammed, G.J., Qi, Z.-Y., 2017. Responses of plant proteins to heavy metal stress—a review. Front. Plant Sci. 8, 1492. http://dx.doi.org/10.3389/fpls.2017.01492.

Havir, E.A., Mchale, N.A., 1987. Biochemical and developmental characterization of multiple forms of catalase in tobacco leaves. Plant Physiol. 84, 450–455. http://dx.doi.org/10.1104/pp.84.2.450.

Hayat, S., Khalique, G., Irfan, M., Wani, A.S., Tripathi, B.N., Ahmad, A., 2012. Physiological changes induced by chromium stress in plants: an overview. Protoplasma 249, 599–611. http://dx.doi.org/10.1007/s00709-011-0331-0.

Herrmann, L., Felbinger, C., Haase, I., Rudolph, B., Biermann, B., Fischer, M., 2015. Food Profiling: characterization of the Ecuadorean Type CCN-51 of *Theobroma cacao* L. using microsatellite markers. J. Agric. Food Chem. 63, 4539–4544. ⟨https://10.1021/acs.jafc.5b01462⟩.

Hossain, M.A., Piyatida, P., da Silva, J.A.T., Fujita, M., 2012. Molecular mechanism of heavy metal toxicity and tolerance in plants: central role of glutathione in detoxification of reactive oxygen species and methylglyoxal and in heavy metal chelation. J. Bot. 1–37. http://dx.doi.org/10.1155/2012/872875.

Kabata-Pendias, A., 2011. Trace Elements in Soils and Plants. CRC Press, Boca Ratón, Florida, pp. 561.

Khedr, A.H., Abbas, M.A., Wahid, A.A., Quick, W.P., Abogadallah, G.M., 2003. Proline induces the expression of salt-stress-responsive proteins and may improve the adaptation of Pancratium maritimum L. to salt-stress. J. Exp. Bot. 54, 2553–2562. http://dx.doi.org/10.1093/jxb/erg277.

Li, F., Vierstra, R.D., 2012. Autophagy: a multifaceted intracelular system for bulk and selective recycling. Trends Plant Sci. 17, 526–537. http://dx.doi.org/10.1016/j.tplants.2012.05.006.

Lichtenthaler, H.K., Wellburn, A.R., 1983. Determinations of total carotenoids and chlorophylls *a* and *b* of leaf extracts in diferente solventes. Biochem Soc. Trans. 11, 591–592. http://dx.doi.org/10.1042/bst0110591.

Livak, K.J., Schmittgen, T.D., 2001. Analysis of relative gene expression data using real-time quantitative PCR and the 2-ΔΔCt method. Methods 25, 402–408. http://dx.doi.org/10.1006/meth.2001.1262.

López-Luna, J., Gonzalez-Chavez, M., Esparza-Garcia, F., Rodriguez-Vazquez, R., 2009. Toxicity assessment of soil amended with tannery sludge, trivalent chromium and hexavalent chromium, using wheat, oat and sorghum plants. J. Hazard. Mater. 163, 829–834. http://dx.doi.org/10.1016/j.jhazmat.2008.07.034.

Mangabeira, P.A., Ferreira, A.S., Almeida, A.-A.F., Fernandes, V.F., Lucena, E., Souza, V.L., Santos Júnior, A.J., Oliveira, A.H., Grenier-Loustalot, M.F., Barbier, F., 2011. Compartmentalization and ultrastructural alterations induced by chromium in aquatic macrophytes. Biomet. Int. J. Role Met. Ions Biol. Biochem. Med. 24, 1017–1026. http://dx.doi.org/10.1007/s10534-011-9459-9.

Minina, E.A., Bozhkov, P.V., Hofius, D., 2014. Autophagy as initiator or executioner of cell death. Trends Plant Sci. 19, 692–697. http://dx.doi.org/10.1016/j.tplants.2014.07.007.

Mittler, R., 2017. ROS are good. Trends Plant Sci. 22, 11–19. http://dx.doi.org/10.1016/j.tplants.2016.08.002.

Mourato, M., Reis, R., Martins, L.L., 2012. Characterization of plant antioxidative system in response to abiotic stresses: a focus on heavy metal toxicity. In: Montanaro, G. (Ed.), Advances in Selected Plant Physiology Aspects. IntechOpen, London. http://dx.doi.org/10.5772/34557.

Nakano, Y., Asada, K., 1981. Hydrogen peroxide is scavenged by ascorbate-specific peroxidase in spinach chloroplasts. Plant Cell Physiol. 22, 867–880. http://dx.doi.org/10.1093/oxfordjournals.pcp.a076232.

Oliveira, H., 2012. Chromium as an environmental pollutant: insights on induced plant toxicity. J. Bot. http://dx.doi.org/10.1155/2012/375843. (Article. ID 375843).

Paiva, L.B., de Oliveira, J.G., Azevedo, R.A., Ribeiro, D.R., da Silva, M.G., Vitória, A.P., 2009. Ecophysiological responses of water hyacinth exposed to Cr^{3+} and Cr^{6+}. Environ. Exp. Bot. 65, 403–409. http://dx.doi.org/10.1016/j.envexpbot.2008.11.012.

Panda, S.K., Choudhury, S., 2005. Chromium stress in plants. Braz. J. Physiol. 17, 95–102. http://dx.doi.org/10.1590/S1677-04202005000100008.

Pandey, V., Dixit, V., Shyam, R., 2009. Chromium effect on ROS generation and detoxification in pea (*Pisum sativum*) leaf chloroplasts. Protoplasma 236, 85–95. http://dx.doi.org/10.1007/s00709-009-0061-8.

Patnaik, A.R., Achary, V.M.M., Panda, B.B., 2013. Chromium (VI)-induced hormesis and genotoxicity are mediated through oxidative stress in root cells of Allium cepa L. Plant Growth Regul. 71, 157–170. http://dx.doi.org/10.1007/s10725-013-9816-5.

Pirovani, C.P., Carvalho, H.A.S., Machado, R.C.R., Gomes, D.S., Alvim, F.C., Pomella, A.W.V., Gramacho, K.P., Cascardo, J.C.D.M., Pereira, G.A.G., Micheli, F., 2008. Protein extraction for proteome analysis from cacao leaves and meristems, organs infected by *Moniliophthora perniciosa*, the causal agent of the witches' broom disease. Electrophoresis 29, 2391–2401. http://dx.doi.org/10.1002/elps.200700743.

Poschenrieder, C., Cabot, C., Martos, S., Gallego, B., Barceló, J., 2013. Do toxic ions induce hormesis in plants? Plant Sci. 212, 15–25. http://dx.doi.org/10.1016/j.plantsci.2013.07.012.

Prasad, A., Singh, A.K., Chand, S., Chanotiya, C., Patra, D., 2010. Effect of chromium and lead on yield, chemical composition of essential oil, and accumulation of heavy metals of mint species. Commun. Soil Sci. Plant Anal. 41, 2170–2186. http://dx.doi.org/10.1080/00103624.2010.504798.

Rehem, B.C., Almeida, A.-A.F., Santos, I.C., Gomes, F.P., Pirovani, C.P., Romero, P., Botía, P., 2011a. Daily and seasonal patterns of leaf water relations and gas exchange of regulated deficit-irrigated almond trees under semiarid conditions. Environ. Exp. Bot. 56, 158–173. http://dx.doi.org/10.1016/j.envexpbot.2005.01.012.

Rehem, B.C., Almeida, A.-A.F., Santos, I.C., Gomes, F.P., Pirovani, C.P., Mangabeira, P.A.O., Corrêa, R.X., Yamada, M.M., Valle, R.R., 2011b. Photosynthesis, chloroplast ultrastructure, chemical composition and oxidative stress in *Theobroma cacao* hybrids with the lethal gene *luteus-Pa* mutante. Photosynthetica 49 (1), 127–139. http://dx.doi.org/10.1007/s11099-011-0021-3.

Reis, G.S.M., Almeida, A.-A.F., Almeida, N.M., Castro, A.V., Mangabeira, P.A.O., Pirovani, C.P., 2015. Molecular, biochemical and ultrastructural changes induced by Pb toxicity in seedlings of *Theobroma cacao* L. PLoS One 10, e0129696. http://dx.doi.org/10.1371/journal.pone.0129696.

Rodriguez, E., Azevedo, R., Fernandes, P., Santos, C., 2011. Cr (VI) induces DNA damage, cell cycle arrest and polyploidization: a flow cytometric and comet assay study in *Pisum sativum*. Chem. Res. Toxicol. 24, 1040–1047. http://dx.doi.org/10.1021/tx2001465.

Santana, K.B., de Almeida, A.-A.F., Souza, V.L., Mangabeira, P.A.O., Silva, D.D., Gomes, F.B., Dutruch, L., Loguercio, L.L., 2012. Physiological analyses of *Genipa americana* L. reveals a tree with ability as phytostabilizer and rhizofilterer of chromium ions for phytoremediation of polluted watersheds. Environ. Exp. Bot. 80, 35–42. http://dx.doi.org/10.1016/j.envexpbot.2012.02.004.

Scoccianti, V., Bucchini, A.E., Lacobucci, M., Ruiz, K.B., Biondi, S., 2016. Oxidative stress and antioxidant responses to increasing concentrations of trivalent chromium in the Andean crop species *Chenopodium quinoa* Willd. Ecotoxicol. Environ. Saf. 133, 25–35. http://dx.doi.org/10.1016/j.ecoenv.2016.06.036.

Shahid, M., Shamshad, S., Rafiq, M., Khalid, S., Bibi, I., Niazi, N.K., Dumat, C., Rashid, M.I., 2017. Chromium speciation, bioavailability, uptake, toxicity and detoxification in soil-plant system: a review. Chemosphere 178, 513–533. http://dx.doi.org/10.1016/j.chemosphere.2017.03.074.

Shanker, A.K., Cervantes, C., Loza-Tavera, H., Avudainayagam, S., 2005. Chromium toxicity in plants. Environ. Int. 31, 739–753. http://dx.doi.org/10.1016/j.envint.2005.02.003.

Singh, H.P., Mahajan, P., Kaur, S., Batish, D.R., Kohli, R.K., 2013. Chromium toxicity and tolerance in plants. Environ. Chem. Lett. 11, 229–254. http://dx.doi.org/10.1007/s10311-013-0407-5.

Souza, L.V., Almeida, A.-A.F., Souza, J.S., Mangabeira, P.A.O., Jesus, R.M., Pirovani, C.P., Ahnert, D., Baligar, V., Loguercio, L.L., 2014. Altered physiology, cell structure, and gene expression of *Theobroma cacao* seedlings subjected to Cu toxicity. Environ. Sci. Pollut. Res. 21, 1217. http://dx.doi.org/10.1007/s11356-013-1983-4.

Souza Júnior, J.O., Carmello, Q.A.C., Sodré, G.A., 2011. Substrato e adubação fosfatada para a produção de mudas clonais de cacau. Rev. Bras. Ciênc. Solo 35, 151–159. http://dx.doi.org/10.1590/S0100-06832011000100014. [Online].

Srivastava, V., Sarkar, A., Singh, S., Singh, P., de Araujo, A.S.F., Singh, R.P., 2017. Agroecological responses of heavy metal pollution with special emphasis on soil health and plant performances. Front. Environ. Sci. 5, 64. ⟨https://http://dx.doi.org/10.3389/fenvs.2017.00064⟩.

Taiz, L., Zeiger, E., Møller, I.M., Murphy, A., 2017. Fisiologia e desenvolvimento 6 Artmed, Porto Alegre.

Tang, J., Xu, J., Wu, Y., Li, Y., Tang, Q., 2012. Effects of high concentration of chromium stress on physiological and biochemical characters and accumulation of chromium in tea plant (*Camellia sinensis* L.). Afr. J. Biotechnol. 11, 2248–2255. http://dx.doi.org/10.5897/AJB11.2402.

Torres, C.A., Andrews, P.K., Davies, N.M., 2006. Physiological and biochemical responses of fruit exocarp of tomato (*Lycopersicon esculentum* Mill.) mutants to natural photo-oxidative conditions. J. Exp. Bot. 57, 1933–1947. http://dx.doi.org/10.1093/jxb/erj136.

Tripathi, B.N., Singh, V., Ezaki, B., Sharma, V., Gaur, J.P., 2013. Mechanism of Cu-and Cd-induced proline hyperaccumulation in *Triticum aestivum* (wheat). J. Plant Growth Regul. 32, 799–808. http://dx.doi.org/10.1007/s00344-013-9343-7.

UdDin, I., Bano, A., Masood, S., 2015. Chromium toxicity tolerance of *Solanum nigrum L.* and *Parthenium hysterophorus* L. plants with reference to ion pattern, antioxidation activity and root exudation. Ecotoxicol. Environ. Saf. 113, 271–278. http://dx.doi.org/10.1016/j.ecoenv.2014.12.014.

Vaahtera, L., Brosché, M., Wrzaczek, M., Kangasjärvi, J., 2014. Specificity in ROS signaling and transcript signatures. Antioxid. Redox Signal. 21, 1422–1441. http://dx.doi.org/10.1089/ars.2013.5662.

Vicent, J.B., 2017. New evidence against chromium as an essential trace element. J. Nutr. 147, 2212–2219. http://dx.doi.org/10.3945/jn.117.255901.

Yanus, R.L., Sela, H., Borojovich, E.J.C., Zakon, Y., Saphier, M., Nikolski, A., Gutflais, E., Lorber, A., Karpas, Z., 2014. Trace elements in cocoa solids and chocolate: an ICPMS study. Talanta 119, 151–154. http://dx.doi.org/10.1016/j.talanta.2013.10.048.

Zheng, L., Peer, T., Seybold, V., Lütz-Meindl, U., 2012. Pb-induced ultrastructural alterations and subcellular localization of Pb in two species of Lespedeza by TEM-coupled electron energy loss spectroscopy. Environ. Exp. Bot. 77, 196–206. http://dx.doi.org/10.1016/j.envexpbot.2011.11.018.